

Removing cross-phase modulation from midinfrared chirped-pulse upconversion spectra

Kevin Lee, Patrick Nuernberger, Adeline Bonvalet, Manuel Joffre

► **To cite this version:**

Kevin Lee, Patrick Nuernberger, Adeline Bonvalet, Manuel Joffre. Removing cross-phase modulation from midinfrared chirped-pulse upconversion spectra. *Optics Express*, Optical Society of America - OSA Publishing, 2009, 17 (21), pp.18738-18744. 10.1364/OE.17.018738 . hal-00818492

HAL Id: hal-00818492

<https://hal-polytechnique.archives-ouvertes.fr/hal-00818492>

Submitted on 14 May 2014

HAL is a multi-disciplinary open access archive for the deposit and dissemination of scientific research documents, whether they are published or not. The documents may come from teaching and research institutions in France or abroad, or from public or private research centers.

L'archive ouverte pluridisciplinaire **HAL**, est destinée au dépôt et à la diffusion de documents scientifiques de niveau recherche, publiés ou non, émanant des établissements d'enseignement et de recherche français ou étrangers, des laboratoires publics ou privés.

Removing cross-phase modulation from midinfrared chirped-pulse upconversion spectra

Kevin F. Lee, Patrick Nuernberger, Adeline Bonvalet and Manuel Joffre*

*Laboratoire d'Optique et Biosciences, Ecole Polytechnique
Centre National de la Recherche Scientifique, 91128 Palaiseau, France
Institut National de la Santé et de la Recherche Médicale, U696, 91128 Palaiseau, France
manuel.joffre@polytechnique.edu

Abstract: We observe that narrow spectral features in mid-infrared spectra obtained by chirped-pulse up-conversion are strongly distorted by cross-phase modulation between the mid-infrared field and the chirped pulse. We discuss the consequences of this effect on spectral resolution, and introduce a correction method that recovers masked lines. This simple correction can be applied either when the upconverted field is fully characterized, such as in multidimensional spectroscopy, or when causality can be used, such as in absorption spectroscopy, which we demonstrate experimentally.

©2009 Optical Society of America

OCIS codes: (190.7220) Upconversion; (300.6340) Spectroscopy, infrared.

References and links

1. E. J. Heilweil, "Ultrashort-pulse multichannel infrared spectroscopy using broadband frequency conversion in LiIO_3 ," *Opt. Lett.* **14**(11), 551–553 (1989).
2. K. J. Kubarych, M. Joffre, A. Moore, N. Belabas, and D. M. Jonas, "Mid-infrared electric field characterization using a visible charge-coupled-device-based spectrometer," *Opt. Lett.* **30**(10), 1228–1230 (2005).
3. M. F. DeCamp, and A. Tokmakoff, "Upconversion multichannel infrared spectrometer," *Opt. Lett.* **30**(14), 1818–1820 (2005).
4. T. P. Dougherty, and E. J. Heilweil, "Dual-beam subpicosecond broadband infrared spectrometer," *Opt. Lett.* **19**(2), 129–131 (1994).
5. J. Treuffet, K. J. Kubarych, J.-C. Lambry, E. Pilet, J.-B. Masson, J.-L. Martin, M. H. Vos, M. Joffre, and A. Alexandrou, "Direct observation of ligand transfer and bond formation in cytochrome c oxidase by using mid-infrared chirped-pulse upconversion," *Proc. Natl. Acad. Sci. U.S.A.* **104**(40), 15705–15710 (2007).
6. M. F. DeCamp, L. P. Deflores, K. C. Jones, and A. Tokmakoff, "Single-shot two-dimensional infrared spectroscopy," *Opt. Express* **15**(1), 233–241 (2007).
7. M. J. Nee, R. McCanne, K. J. Kubarych, and M. Joffre, "Two-dimensional infrared spectroscopy detected by chirped pulse upconversion," *Opt. Lett.* **32**(6), 713–715 (2007).
8. M. J. Nee, C. R. Baiz, J. M. Anna, R. McCanne, and K. J. Kubarych, "Multilevel vibrational coherence transfer and wavepacket dynamics probed with multidimensional IR spectroscopy," *J. Chem. Phys.* **129**(8), 084503 (2008).
9. T. Witte, D. Zeidler, D. Proch, K. L. Kompa, and M. Motzkus, "Programmable amplitude- and phase-modulated femtosecond laser pulses in the mid-infrared," *Opt. Lett.* **27**(2), 131–133 (2002).
10. H.-S. Tan, E. Schreiber, and W. S. Warren, "High-resolution indirect pulse shaping by parametric transfer," *Opt. Lett.* **27**(6), 439–441 (2002).
11. C. Schrieber, S. Lochbrunner, M. Optiz, and E. Riedle, "19 fs shaped ultraviolet pulses," *Opt. Lett.* **31**(4), 543–545 (2006).
12. P. Nuernberger, G. Vogt, R. Selle, S. Fechner, T. Brixner, and G. Gerber, "Generation of shaped ultraviolet pulses at the third harmonic of titanium-sapphire femtosecond laser radiation," *Appl. Phys. B* **88**(4), 519–526 (2007).
13. L. J. Richter, T. P. Petrali-Mallow, and J. C. Stephenson, "Vibrationally resolved sum-frequency generation with broad-bandwidth infrared pulses," *Opt. Lett.* **23**(20), 1594–1596 (1998).
14. T. Ishibashi, and H. Onishi, "Vibrationally resonant sum-frequency generation spectral shape dependent on the interval between picosecond-visible and femtosecond-infrared laser pulses," *Chem. Phys. Lett.* **346**(5-6), 413–418 (2001).
15. G. W. Jones, D. L. Marks, C. Vinegoni, and S. A. Boppart, "High-spectral-resolution coherent anti-Stokes Raman scattering with interferometrically detected broadband chirped pulses," *Opt. Lett.* **31**(10), 1543–1545 (2006).
16. L. Lepetit, G. Cheriaux, and M. Joffre, "Linear techniques of phase measurement by femtosecond spectral interferometry for applications in spectroscopy," *J. Opt. Soc. Am. B* **12**(12), 2467–2474 (1995).

17. A. W. Albrecht, J. D. Hybl, S. M. Gallagher Faeder, and D. M. Jonas, "Experimental distinction between phase shifts and time delays: Implications for femtosecond spectroscopy and coherent control of chemical reactions," *J. Chem. Phys.* **111**(24), 10934–10956 (1999).
18. C. Dorrer, N. Belabas, J. P. Likforman, and M. Joffre, "Spectral resolution and sampling issues in Fourier-transform spectral interferometry," *J. Opt. Soc. Am. B* **17**(10), 1795–1802 (2000).
19. N. Jacquinet-Hussonn, N. Scott, A. Chedina, L. Crepeau, R. Armante, V. Capelle, J. Orphal, A. Coustenis, C. Bonne, N. Poulet-Crovisier, A. Barbee, M. Birk, L. Brown, C. Camy-Peyret, C. Claveau, K. Chance, N. Christidis, C. Clerboux, P. Coheur, V. Dana, L. Daumont, M. D. Backer-Barilly, G. D. Lonardo, J. Flaud, A. Goldman, A. Hamdouni, M. Hess, M. Hurley, D. Jacquemart, I. Kleiner, P. Kopke, J. Mandin, S. Massie, S. Mikhailenko, V. Nemtchinov, A. Nikitin, D. Newnham, A. Perrin, V. Perevalov, S. Pinnock, L. Regalia-Jarlot, C. Rinsland, A. Rublev, F. Schreier, L. Schult, K. Smith, S. Tashkun, J. Teffo, R. Toth, V. Tyuterev, J. Auwera, P. Varanasi, and G. Wagner, "The GEISA spectroscopic database: Current and future archive for earth and planetary atmosphere studies," *J. Quant. Spectrosc. Radiat. Transf.* **109**(6), 1043–1059 (2008).
20. P. Nuernberger, K. F. Lee, A. Bonvalet, T. Polack, M. H. Vos, A. Alexandrou, and M. Joffre, "Suppression of perturbed free induction decay and noise in experimental ultrafast pump-probe data," *Opt. Lett.* (to be published).
21. C. Iaconis, and I. A. Walmsley, "Spectral phase interferometry for direct electric-field reconstruction of ultrashort optical pulses," *Opt. Lett.* **23**(10), 792–794 (1998).
22. J. Wemans, G. Figueira, N. Lopes, and L. Cardoso, "Self-referencing spectral phase interferometry for direct electric-field reconstruction with chirped pulses," *Opt. Lett.* **31**(14), 2217–2219 (2006).
23. B. von Vacano, T. Buckup, and M. Motzkus, "Shaper-assisted collinear SPIDER: fast and simple broadband pulse compression in nonlinear microscopy," *J. Opt. Soc. Am. B* **24**(5), 1091–1100 (2007).

1. Introduction

Various methods have been demonstrated for measuring mid-infrared (mid-IR) femtosecond pulses directly with a visible detector [1–3], and have been subsequently applied to pump-probe [4,5] and multidimensional [6–8] mid-IR spectroscopy. One of these methods, chirped-pulse up-conversion (CPU) [2], consists of mixing the mid-IR field with a stretched pulse, typically the uncompressed output of a chirped pulse amplifier. Although reported CPU applications [5,7,8] were associated with moderate spectral resolution, this method has the potential for extremely high spectral resolution, given the long duration of the chirped pulse and the high pixel count of silicon-based charge-coupled device (CCD) cameras.

The simple view of CPU is the uniform addition of a constant local frequency from the chirped pulse to the signal field. For narrow spectral features, there must be long features in time. In this case, there will be a range of wavelengths, or equivalently, nonlinear phase variations, with which the signal field mixes. This results in phase modulation, and thus spectral broadening. The narrower the spectral feature, the greater the distortion.

The same effect limits indirect pulse shaping techniques where a shaped pulse is mixed with a chirped pulse to transfer the shape to the mid-IR [9,10] or the ultraviolet [11,12], because narrow amplitude modulations cannot be transferred without adjacent spectral oscillations. The same is true if narrow spectral features in spectroscopy are measured after a nonlinear interaction with a chirped pulse, such as in vibrationally-resolved sum-frequency generation [13,14], and coherent anti-Stokes Raman scattering (CARS) with chirped pump pulses [15].

In the chirped pump pulse CARS case, the anti-Stokes pulse was characterized in amplitude and phase, and the phase modulation removed [15]. This will also work for multidimensional spectroscopy, where the upconverted pulse is usually fully characterized. We will discuss this case, and further extend the correction to cases when the field is not fully characterized. By making use of causality, cases such as pump-probe absorption spectroscopy can be corrected, greatly improving the spectral resolution.

2. Upconversion and the phase of the chirped pulse

To estimate when the chirp is important, we consider the balance between the resolution limit from the spectral feature itself, which can be modeled as a transform-limited Gaussian pulse, and from the chirped pulse. These two contributions are of equal magnitude when the change in instantaneous frequency of the chirped pulse over the duration of the model pulse is comparable to the spectral width of the model pulse. For our chirped pulse, the second-order

derivative of the spectral phase at the central frequency ω_0 is $\varphi'' \approx 4 \text{ ps}^2$, which corresponds to a spectral resolution of about 6 cm^{-1} (full width at half maximum (FWHM)).

Let us call $E(t)$ the mid-IR field incident on the nonlinear upconversion crystal, where it is mixed with a stretched pulse of center frequency ω_0 (assumed to overlap with the mid-IR field at $t = 0$). For simplicity, we assume a thin nonlinear crystal, so that phase matching issues can be ignored, and that the relative bandwidth of the upconverted field is small enough so that the field radiated by the crystal is simply proportional to the term of interest of the nonlinear polarization, itself proportional to the time-domain product of the mid-IR field $E(t)$ and the chirped field $A(t)\exp(-i\omega_0 t + i\Phi(t))$. We thus have

$$E_{\text{cpu}}(t) = \eta E(t) e^{-i\omega_0 t} A(t) e^{i\Phi(t)} \quad (1)$$

where η is a coefficient including, among other terms, the second-order nonlinear coefficient of the crystal and the $\pi/2$ phase shift between the polarization and the radiated field. $A(t)$ is a real quantity proportional to the envelope of the chirped-pulse field, having a maximum value of 1 which occurs at $t = 0$, when the two pulses are overlapped. In our case, we can approximate the spectral phase of the chirped pulse to be only second order, as our third order dispersion (-0.015 ps^3) does not significantly affect the correction. The time-domain phase is then parabolic and, in the case of a sufficiently large chirp, $\Phi(t) = -t^2 / (2\varphi'')$ [12,15]. The mid-IR field is thus multiplied by three time-dependent terms. The multiplication by the first term, $\exp(-i\omega_0 t)$, corresponds to a translation in frequency space, the desired effect from CPU. The multiplication by $A(t)$ will result in a convolution in frequency domain and will therefore limit the spectral resolution. However, if the stretching factor is greater than 1000 (which is true in most chirped pulse amplifiers) this corresponds to a spectral resolution better than a thousandth of the pulse bandwidth and will be of the order of one pixel or less of the CCD camera, making it negligible in the context of this article. The main distortion in the field results from the multiplication with the last term, $\exp(i\Phi(t))$. This phase modulation in time can severely distort the spectrum by inducing spectral oscillations and broadening.

3. Multidimensional spectroscopy

The phase modulation described in the previous section can be easily corrected if the spectral amplitude and phase of the upconverted pulse is known. The electric field can then be calculated in time domain, where the parabolic phase of the chirped pulse can be readily removed [15]. For example, in 2DIR spectroscopy, the mid-IR emission from the sample interferes with a reference pulse, allowing a complete amplitude and phase determination using Fourier-transform spectral interferometry (FTSI) [16–18]. We consider here the CPU implementation of 2DIR spectroscopy [7], where the mid-IR field incident on the upconversion nonlinear crystal is the superposition of a reference field $E_{\text{ref}}(t)$ and of a signal field $E_s(t)$ that needs to be measured. The reference pulse is assumed to be nearly transform limited whereas the signal field can have an arbitrary duration. The upconverted field reads $E_{\text{cpu}}(t) = E_{\text{ref,cpu}}(t) + E_{\text{s,cpu}}(t)$, where the CPU fields are related to the mid-IR fields through Eq. (1). In the case of the reference field, which is nearly transform limited and hence much shorter than the chirped pulse, we have $A(t) \approx 1$ and $\Phi(t) \approx 0$, for t where $E_{\text{ref}}(t)$ is non-negligible, so that $E_{\text{ref,cpu}}(t) \approx \eta E_{\text{ref}}(t) \exp(-i\omega_0 t)$. Therefore, the upconverted reference pulse is not subject to phase modulation and is simply a translated replica of the mid-IR reference field. Using FTSI, it is possible to extract $E_{\text{ref,cpu}}^*(\omega) E_{\text{s,cpu}}(\omega)$ after a pair of Fourier transforms [16]. Dividing by the complex reference field then yields the CPU field $E_{\text{s,cpu}}(\omega)$, and then $E_{\text{s,cpu}}(t)$ after an additional Fourier transform. The parabolic phase $\Phi(t)$ can then be subtracted to yield after a final inverse Fourier transform the undistorted mid-IR field $E_s(\omega)$.

It is possible to combine these transforms. The first Fourier transform of the spectral interferogram extracts the correlation product $E_{\text{ref,cpu}}^*(-t) \otimes E_{\text{s,cpu}}(t)$, where \otimes is the convolution product. This quantity is reasonably close to $E_{\text{s,cpu}}(t)$ if the reference pulse is nearly transform limited. The phase term $\Phi(t)$ can then be directly subtracted from the

correlation product, and an inverse Fourier transform directly yields the product of $E_{\text{ref}}^*(\omega)$ with the corrected mid-IR field.

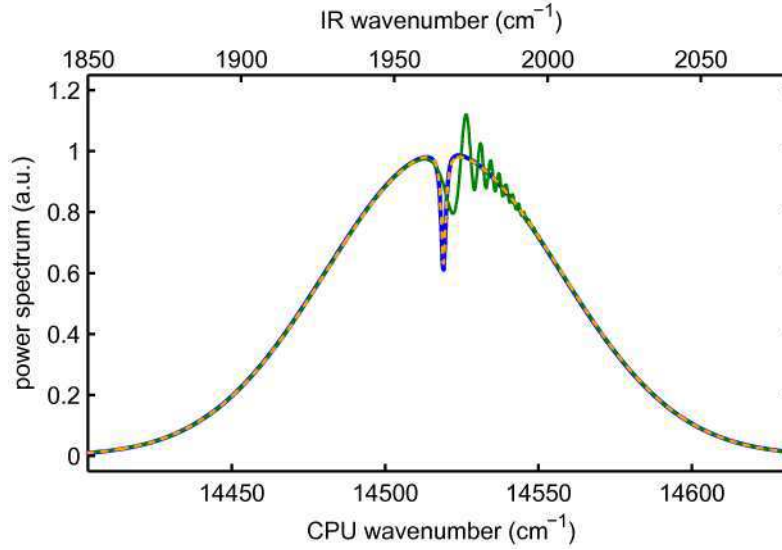


Fig. 1. Simulated spectrum (orange dashes) of a Gaussian pulse (FWHM 90 cm^{-1} , centered at 1966 cm^{-1}) transmitted through a Lorentzian absorption line (0.2 OD at peak and FWHM = 1.6 cm^{-1}) under the assumption of upconversion with a monochromatic field at 12553 cm^{-1} . The lower x-axis corresponds to the wavenumber measured after upconversion, the upper x-axis to the one in the mid-IR. The oscillating green curve shows the simulated CPU spectrum obtained with a chirped upconversion pulse (FWHM 136 cm^{-1} , centered at 12553 cm^{-1} and having $\phi'' = 3.9 \text{ ps}^2$). The blue curve shows the absorption spectrum retrieved from the CPU spectrum using the procedure described in the text.

4. Absorption spectroscopy

Let us now consider the case of absorption spectroscopy, either in the linear transmission regime or in a pump-probe configuration. We will show that although the field is not completely characterized in this case, a correction procedure similar to that introduced in the previous section can still be applied. In analogy with the Kramers-Kronig relations, the method relies on the causality principle. Let us call $E_{\text{pr}}(t)$ the field of the incident probe pulse and $E_s(t)$ the field radiated by the sample. The incident probe pulse is assumed to be nearly transform limited and centered on $t = 0$. However, the radiated field $E_s(t)$ is zero before excitation, that is, negative times earlier than a few probe pulse durations, and can be arbitrarily long for positive times, depending on the dephasing times of the sample. The mid-IR spectrum reads

$$I(\omega) = |E_{\text{pr}}(\omega) + E_s(\omega)|^2 \approx |E_{\text{pr}}(\omega)|^2 + E_{\text{pr}}^*(\omega)E_s(\omega) + E_{\text{pr}}(\omega)E_s^*(\omega), \quad (2)$$

assuming small absorption, with $|E_s(\omega)|^2$ much smaller than the spectral intensity of the incident probe pulse. As in homodyne detection, absorption results from the interference between the incident field and the radiated field, the last two terms of Eq. (2). After upconversion, we actually measure

$$I_{\text{cpu}}(\omega) \approx |E_{\text{pr,cpu}}(\omega)|^2 + E_{\text{pr,cpu}}^*(\omega)E_{s,\text{cpu}}(\omega) + E_{\text{pr,cpu}}(\omega)E_{s,\text{cpu}}^*(\omega). \quad (3)$$

Due to the phase modulation in $E_{s,\text{cpu}}(t)$, the transmitted spectrum can be severely distorted. Figure 1 shows a simulation of the mid-IR spectrum transmitted through a narrow Lorentzian absorption line (orange curve) as compared to the spectrum that would be measured using

CPU (green curve). Instead of a narrow absorption profile, the CPU spectrum shows strong oscillations on the high-energy side of the absorption frequency. Indeed, the exponentially-decaying radiated field will mix not only with the single frequency ω_0 at $t = 0$ but also with higher frequencies present at later times in the chirped pulse, producing blue-shifted upconverted radiation. The oscillations result from the constructive or destructive interferences between this upconverted radiation and that produced from the mixing between ω_0 and the incident broadband probe pulse.

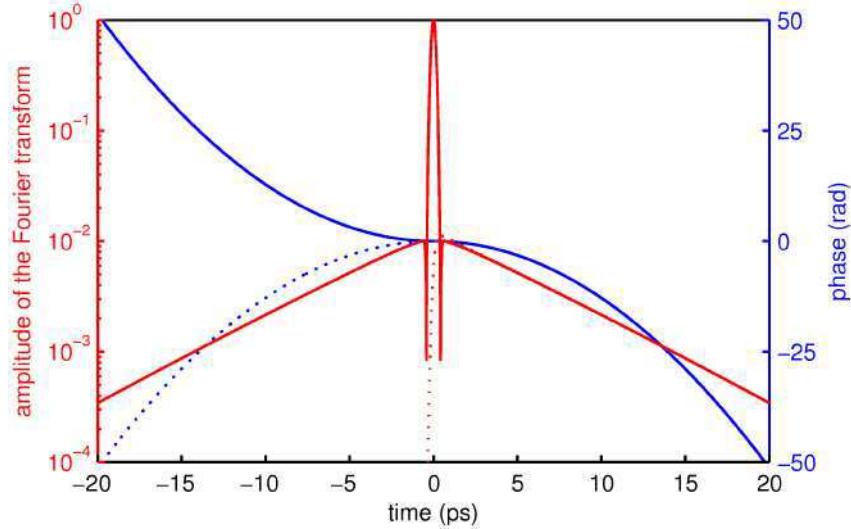


Fig. 2. The solid red line (left vertical axis) shows the amplitude of the Fourier transform of the spectral intensity, $|[FT I_{cpu}(\omega)](t)|$, with the same parameter values as in Fig. 1. The red dotted line shows the contribution of the second term of Eq. (4). The dotted blue line (right vertical axis) shows the time-dependent phase $\Phi(t)$ of the chirped pulse. The solid blue line shows the time-dependent phase $\Phi_{corr}(t)$ used in the data processing.

We now show that these oscillations can be removed by an appropriate processing in Fourier space similar to that of the previous section. A Fourier transform of Eq. (3) yields

$$[FT I_{cpu}(\omega)](t) \approx E_{pr,cpu}(-t) \otimes E_{pr,cpu}(t) + E_{pr,cpu}^*(-t) \otimes E_{s,cpu}(t) + E_{pr,cpu}(t) \otimes E_{s,cpu}^*(-t). \quad (4)$$

Unlike with spectral interferometry, these three terms are overlapping and it is impossible to extract exactly any one of them. However, the key point is that the overlapping region is limited to the immediate vicinity of $t = 0$, where the effect of phase modulation is negligible and no correction is needed. For positive values of time greater than the probe pulse duration, causality implies that only the second term of Eq. (4) will contribute (see Fig. 2), so that the phase correction can be applied simply by subtracting $\Phi(t)$ from the correlation product, as in the previous section. For large negative times, it is the third term in Eq. (4), the time reversed and phase conjugate correlation product, which contributes, so that we need to subtract $-\Phi(-t)$ to correct for the phase modulation. As illustrated in Fig. 2, the phase modulation correction can be performed by subtracting the following phase

$$\Phi_{corr}(t) = \Phi_{corr}(|t|) \text{sign}(t) \quad (5)$$

from the Fourier transform of the measured spectrum, where $\text{sign}(t)$ is the sign function. The fact that this procedure includes an unwanted correction around $t = 0$ is unimportant since $\Phi_{corr}(t)$ takes negligible values in this area due to its quadratic variation with time.

The blue curve in Fig. 1 has been obtained from $I_{\text{cpu}}(\omega)$ (the green curve) by applying this numerical processing, namely a Fourier transform, a subtraction of the phase term $\Phi_{\text{corr}}(t)$, and an inverse Fourier transform. It is very close to the original transmitted spectrum (orange curve). We have observed that the small discrepancy observed at the absorption dip, attributed to the contribution of $|E_{\text{cpu}}(\omega)|^2$ that was not included in our analysis, vanishes when the absorption strength is reduced.

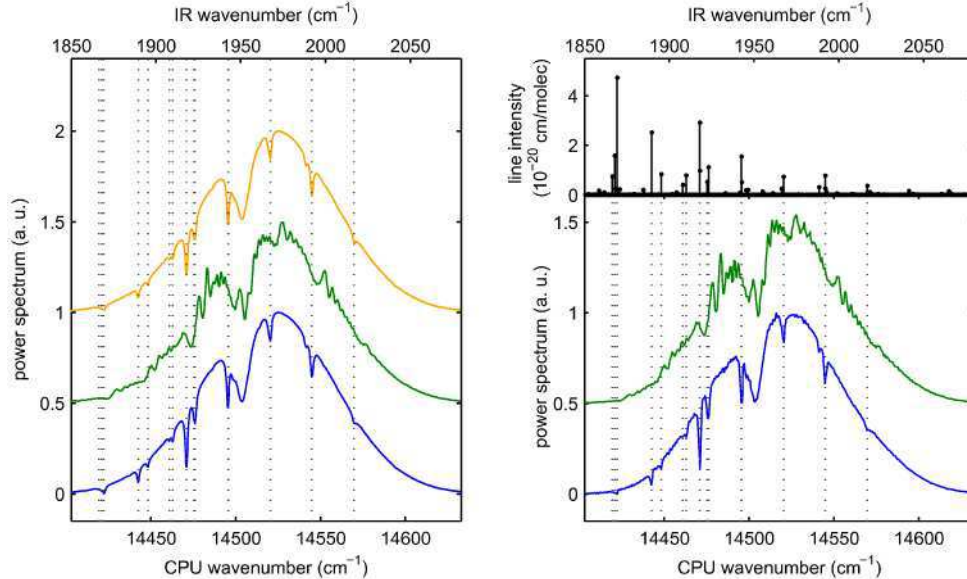


Fig. 3. Simulated (left) and measured (right) normalized mid-IR spectra resulting from transmission through water vapor and HbCO, vertically offset for clarity. From upper to lower curves: the orange curve shows the theoretical mid-IR spectrum expected for a Gaussian pulse (FWHM 90 cm^{-1}) centered at 1966 cm^{-1} , upconverted with a monochromatic light field at 12553 cm^{-1} . The green curve shows the simulated (left) and measured (right) CPU spectrum obtained with a chirped pulse (FWHM 136 cm^{-1} , centered at 12553 cm^{-1} and having $\varphi'' = 3.9\text{ ps}^2$). The blue curves show the spectra obtained by applying the correction procedure described in section 4, evidencing an excellent retrieval of the correct mid-IR spectrum. The water vapor absorption frequencies and relative strengths (shown in the top-right inset) are from the GEISA database [19], the narrow water linewidths were set to our 1.6 cm^{-1} FWHM spectrometer resolution, while the absolute absorption value has been matched to the data. The linewidth of the 1951 cm^{-1} HbCO absorption (9.2 cm^{-1} FWHM for a Lorentzian) has been deduced from perturbed free-induction decay measurements [20]. The measured spectrum is taken with a single laser shot. Dotted gridlines are shown for the 16 most intense lines.

5. Experimental demonstration

We now turn to the experimental demonstration of the correction procedure introduced in this article. Our source is a Ti:Sapphire regenerative amplifier with a 1 kHz repetition rate which drives an optical parametric amplifier, the signal and idler of which undergo difference frequency generation to produce mid-IR pulses. Detection is done by upconversion with uncompressed pulses from the amplifier. This brings the mid-IR pulses into the visible range, where they are detected by an imaging grating spectrometer and CCD array, which records the spectrum for each pulse [2,5].

We have measured the spectrum of our mid-IR laser beam after transmission through 1.87 m of atmosphere. We use the narrow absorption lines of the ambient water vapor to test the correction procedure. We have additionally inserted a $100\mu\text{m}$ thick carboxyhemoglobin (HbCO) sample (5 mM in a Tris-HCl D_2O buffer at $\text{pD}=7.6$, put under CO atmosphere after addition of an excess of dithionite) in the beam to measure simultaneously the CO absorption. Small oscillations ($\approx 2\%$) were present in the measured spectrum due to a replica pulse, and

were filtered out in Fourier space for times between 19.5 and 20.5 ps before Fourier transforming back to the frequency domain.

In Fig. 3, the green curve on the right shows the experimentally measured CPU spectrum for air and HbCO of a single laser shot. While the broader HbCO absorption line is still visible in the experimental CPU spectrum, the narrow absorption lines of water vapor are entirely destroyed by phase modulation. Like Fig. 1, each narrow absorption line gives rise to strong spectral oscillations, with complicated spectra in regions with several neighbouring absorption lines. The measured CPU spectrum is in excellent agreement with calculation (green curve on the right) based on the GEISA database [19] for the frequency and relative strengths of the absorption lines of water vapor. Since these water lines are very narrow [19], our simulation uses water linewidths set to the limiting 1.6 cm^{-1} FWHM resolution of our spectrometer. Figure 3 clearly shows that CPU spectra require the phase correction when measuring narrow spectral features.

Although the pixels are not evenly spaced in frequency, we found that a direct fast Fourier transform (FFT) of the experimental data for the correction of section 4 was nearly identical to that found after Fourier interpolation to a uniform frequency grid [18]. Indeed, the issue of non-uniform pixel spacing in frequency domain is greatly reduced when using CPU, since detection in the visible domain reduces the relative bandwidth by almost one order of magnitude relative to direct detection with a mid-IR detector array. Therefore, we simply computed a FFT of the data, subtracted the phase $\Phi_{\text{corr}}(t)$ (see Eq. (5) with the known value of $\varphi'' = 3.9 \text{ ps}^2$ for our chirped pulse, and computed an inverse FFT to retrieve the corrected spectrum. This processing is simple enough for acquisition software to display corrected spectra in real time. Figure 3 demonstrates the efficacy of the correction. In both the experiment and simulation, the retrieved mid-IR spectra (blue curves) match the theoretical mid-IR spectrum (orange curve), the main difference resulting from the fact that the experimental mid-IR pulse is not exactly Gaussian. Also note that the calibration of the mid-IR frequency axis can be done very accurately using these water absorption lines.

6. Conclusion

We have shown that the spectral resolution in CPU mid-IR spectroscopy, especially for narrow spectral lines, can be vastly improved by a phase correction which compensates for the time dependent phase of the chirped pulse. The correction can remove the distortions from most practical implementations of CPU, when the field is entirely known, as in 2DIR spectroscopy, or when causality can be used, as in absorption spectroscopy.

We have applied our correction to the narrow and broad spectral lines of a mid-IR pulse transmitted through water vapor and HbCO, finding excellent agreement with simulations. For simplicity, we only included the parabolic time dependent phase of the chirped pulse, but higher order terms can be easily included in the correction. The spectral resolution can be further improved by including effects such as higher order dispersion, or intensity variation of the chirped pulse in the correction, $A(t)\exp(i\Phi(t))$ (while taking care not to add noise from the edges of the spectrum). Resolution would then be limited by the number of pixels on the CCD camera and the duration of the chirped pulse. These corrections may also be very useful for other techniques employing frequency-mixing with a chirped pulse, such as spectral phase interferometry for direct electric-field reconstruction [21], where the field retrieval might be improved by removing the phase modulation from the chirped pulse [22,23].

Acknowledgements

We wish to thank Antigoni Alexandrou and Kevin J. Kubarych for highly stimulating discussions on the ultimate limitations of chirped-pulse up-conversion. This work was supported by Agence Nationale de la Recherche (ANR-BLAN-0286). P.N. acknowledges financial support from the Deutsche Akademie der Naturforscher Leopoldina (BMBF-LPDS 2009-6).